Modeling the Heat Treatment of a Starch Suspension Inside a Tubular Exchanger

A. Plana-Fattori[1,2,*], E. Chantoiseau[1,2], C. Doursat[1,2] and D. Flick[1,2]
1: AgroParisTech, UMR1145 Ingénierie Procédés Aliments, F-91300 Massy, France (#)
2: INRA, UMR1145 Ingénierie Procédés Aliments, F-91300 Massy, France (§)
* Corresponding author: Artemio Plana-Fattori, AgroParisTech, Département MMIP, 16 rue Claude Bernard, 75231 Paris, France, artemio.planafattori@agroparistech.fr
# AgroParisTech: Paris Institute of Technology for Life, Food and Environmental Sciences
§ INRA: French National Institute for Agricultural Research

Abstract: Many liquid food processes involve coupled phenomena of fluid flow, heat transfer and product transformation. Fluid flow and heat transfer drive the temperature field; temperature influences the product transformation, which in turn modifies the product viscosity and therefore the fluid flow behavior. In this study a numerical model was developed for coupling these phenomena in the case of a starch suspension inside a tubular heat exchanger. Conservation equations for the fluid mass, momentum and energy were coupled with a second-order kinetics equation representing the swelling of starch granules. These equations were solved under steady-state conditions with the help of the simulation package COMSOL Multi-physics. Velocity and temperature fields were analyzed in view of the local state of food product properties like the mean diameter of starch granules and the suspension viscosity. Our results show that the local present temperature does not drive alone the present food product transport properties.

Keywords: fluid flow, heat transfer, starch granule swelling, coupled numerical model, tubular heat exchanger

1. Introduction

Numerical modeling of fluid flow and heat transfer inside liquid food process equipments has been largely developed (e.g., Norton and Sun, 2006, Kumar and Dilber, 2007). Transport phenomena properties, including the viscosity, are frequently assumed to be a function of the local present temperature. Food transformation processes like starch gelatinization are more rarely taken into account.

Starch is the most widely employed thickener in the food industry. Most industrial processes involve temperatures that can be high enough for enabling starch phase transitions. The concept of "gelatinization" refers to the destruction of the crystalline structure in starch granules; such a process includes, in a broad sense and in time sequence, granular swelling, native crystalline melting and molecular solubilization (Liu et al. 2009).

Liao et al. (2000) studied the continuous flow sterilization of a starch dispersion in which gelatinization is taken into account with the help of a thermo-rheological model. In their model, the mixture viscosity depends on the local present temperature, including two effects: with heating, the apparent viscosity increases due to the starch granule's swelling, whereas the continuous phase viscosity decreases. Implicitly, that model assumes that the starch granules swelling state is a function of the local present temperature only.

Experimental work has shown that the rheological properties of a fluid product can be affected by its thermal history; this is the case of waxy crude oil (Silva and Coutinho, 2004) and selected liquid crystalline polymers (Done and Baird, 2004). We argue that the suspension viscosity associated with a starch dispersion can exhibit a non-negligible dependence on the thermal history of fluid particles. Inside a tubular exchanger, fluid particles running close to the heating wall evolve under thermal and kinetic conditions that can be different from those associated with particles moving faster at greater distances from such wall.

In the present work, the influence of the continuous phase (water) viscosity on the suspension viscosity is separated from the influence due to the starch granule's solid volume fraction. Finite-element-based coupled simulations are conducted with the package COMSOL Multi-physics, including a thermo-kinetic model based on the experimental work of Lagarrigue et al. (2008) about a modified waxy maize starch suspension.

2. Methods

The food product is an aqueous suspension of starch: because its high content of water, it is assumed to be a Newtonian liquid. Density and thermal properties are approximated by those associated with pure water. Conservation equations for the food product mass, momentum and energy can be written as:

$$\nabla.(\rho \mathbf{u}) = 0 \quad (1)$$

$$\rho (\mathbf{u}.\nabla)\mathbf{u} = \nabla.(-p\mathbf{I} + \eta(\nabla\mathbf{u} + (\nabla\mathbf{u})^T)) \quad (2)$$

$$\rho C_P (\mathbf{u}.\nabla)T = \nabla.(k \nabla T) \quad (3)$$

The double influence of temperature on the food product viscosity is separated as follows. The mixture (or absolute) viscosity η is obtained by multiplying the continuous phase (water) viscosity η_W and the starch granules relative viscosity, which depends on the starch granules swelling state. Various approximations have been proposed for estimating the relative viscosity as a function of the solid volume fraction Φ occupied by the particles. We adopted the model proposed by Thomas (1965) because it provides an increase of η / η_W with Φ that is consistent with the experimental data available for the starch suspension assumed in this study. The product viscosity is expressed as:

$$\eta = \eta_W (1 + a\Phi + b\Phi^2 + c\exp(d\Phi)) \quad (4)$$

where a = 2.5, b = 10.05, c = 0.00273 and d = 16.6 . The solid volume fraction Φ is estimated from the mean volume-weighted diameter D that represents the granules' size:

$$\Phi / \Phi_O = (D / D_O)^3 \quad (5)$$

where Φ_O and D_O characterize the starch granule suspension before any heat treatment. Following Lagarrigue *et al*. (2008), we define the degree of granule swelling S of the starch suspension at a given instant from the respective mean diameter D, and from the mean diameter values before any heat treatment (D_O) and after complete heat treatment (D_M):

$$S = (D - D_O) / (D_M - D_O) \quad (6)$$

Starch granule swelling is evaluated through the following second-order kinetics equation:

$$\mathbf{u}.\nabla S = V(1 - S)^2 + \nabla.(D_S \nabla S) \quad (7)$$

where D_S is the coefficient of diffusivity and V is the rate constant; the latter can be expressed in terms of the Arrhenius law:

$$V(T) = V_O \exp(-E_A / (R T)) \quad (8)$$

where E_A is the activation energy, and R is the gas constant.

Selected starch dispersions have been studied by Lagarrigue *et al*. (2008). Those authors followed the kinetics of granule swelling when applying thermo-mechanical treatments in a laboratory simulator coupled to a rheometer. Data on granule swelling and apparent viscosity development were obtained under controlled temperature and shear conditions. Among the suspensions studied, we focused the attention on the 3.1 % w/w modified waxy maize starch dispersion; it corresponds to D_O = 15.5 and D_M = 39.6 µm, Φ_O = 0.03, V_O = 2.9e+12 s^{-1}, and E_A = 84.8 kJ.mol^{-1} (see Tables 2 and 3, and Fig. 6 of Lagarrigue *et al*., 2008).

The coefficient of diffusion D_S required in equation (7) can be estimated through the analysis of the Brownian motion that takes place in the case of a dilute suspension of spherical colloidal particles (Bird *et al*., 2007):

$$D_S = K T / (3 \pi \eta_W D) \quad (9)$$

where K is the Boltzmann constant and D is the particle diameter. In the case of the modified waxy maize starch dispersion that was studied by Lagarrigue *et al.* (2008), the mean volume-weighted diameters ranged from D_O = 15.5 and D_M = 39.6 µm; it allows D_S values between 1.1 and 4.3e-14 $m^2.s^{-1}$.

The coupled phenomena under consideration are illustrated inside a tubular heat exchanger, with length 1 m and radius 5 mm. Looking forward the numerical model, a two-dimension axial-symmetric domain was built. A uniform flux of 10 $kW.m^{-2}$ is applied on the heating wall, and the temperature associated with the starch dispersion is assumed to be 20 °C at the inlet. These conditions enable a maximum temperature

near the wall at the exchanger outlet of about 91°C, which corresponds to a relevant degree of starch granule swelling (see Table 2 of Lagarrigue *et al*., 2008). A fully developed parabolic flow profile was assumed at the inlet. The flow rate was fixed at 10 liters per hour (mean velocity of 0.035 $m.s^{-1}$). According to the Reynolds number (below 600), the flow regime is laminar.

Conservation equations (1-3) were combined with the second-order kinetics equation (7) and solved with the help of the finite-element-based method. These equations are strongly coupled, and streamline diffusion was applied to the whole system of equations; the Garlekin least-square technique was employed for fluid flow and heat transfer, whereas anisotropic diffusion (with a tuning parameter $\delta = 0.5$) was applied to granule swelling. Because changes in suspension viscosity and therefore in velocity field are expected, crosswind diffusion (with a tuning parameter $C_K = 0.1$) was applied to fluid flow for avoiding a denser mesh. Second-order Lagrange elements were employed in all cases. The Parallel Sparse Direct Linear Solver (PARDISO) was taken into account for solving the problem; it implements an efficient method for large systems of equations like those arising from the finite element method (Schenk and Gartner, 2004).

In developing our numerical coupled model, many tests were performed regarding mainly the mesh resolution and the coefficient of diffusion. Next section discusses the more relevant tests while justifies the choices adopted for these both issues. Computations were carried out with the simulation package COMSOL Multi-physics (version 3.5a) on a 64-bits calculator disposing of 24 Gb of RAM.

3. Results

Sensitivity tests were conducted for assessing the convergence of our results with the increase of the mesh resolution. As emphasized by Kuipers and Swaaij (1998), only computational results that possess invariance with respect to discretization could in a further step be confronted with experimental data. Following tests assess the influence of mesh resolution on: i) mass-weighted estimates at the domain outlet (i.e. candidates for a future observation), and ii) local estimates along the heating wall, where the representation of coupled processes is expected to be challenging.

Figure 1 presents mass-weighted estimates of swelling degree at the outlet as function of the number of cells. Results exhibit an asymptotic behavior as the number of cells increases. Coarser resolutions (less than ~50000 cells) provided unreliable results somewhere in the domain, e.g. local swelling degree higher than the unity. Finer resolutions (more than ~250000 cells) allowed LU factorization out of memory, indicating the limits in applying the PARDISO solver with our present calculation capabilities. Comparisons with other solvers were considered out of scope in this study.

Meshes under consideration are constituted of identical cells characterized by dimensions *dz* and *dr* along the domain's length and radius respectively. We avoided the aspect ratio *dz/dr* = 1 because its high calculation requirements. On the other hand, it is known that too large *dz/dr* values decrease accuracy. In our case, the temperature gradient is mainly oriented along the domain's radius and therefore *dr* has to be small; otherwise, *dz* can be relatively large because the flow is mainly oriented along the domain's length. Selected aspect ratios were assumed in order to compare results obtained with "short-" (*dz/dr* = 2) and "long-rectangles" (= 8), as well as with those associated with two intermediate values (= 4 and 5). Figure 1 shows that the application of distinct aspect ratios allows relatively similar results. Moreover, for meshes constituted of ~250000 cells, results obtained with *dz/dr* = 2, 4, and 5 are relatively closer each other them than with results obtained with *dz/dr* = 8. Following tests are performed with the aspect ratio *dz/dr* = 5.

Figure 2 compares selected variables at the heating wall as function of the distance from the domain's inlet, for a given aspect ratio (*dz/dr* = 5) and different numbers of cells (from 40x1600 = 64000 to 80x3200 = 256000). Red curves correspond to results obtained with the 80x3200-cells mesh; values are displayed on left side. These results show the estimates evolution along the heating wall: almost full swelling takes place after about 1/4 of the tubular exchanger's length, allowing an increase of the suspension viscosity by a factor near to 7. Figure 2 shows that, in the case of the coupled problem under consideration, results at the heating wall can be differently

influenced by the mesh resolution. For instance, by starting with a coarse resolution (40x1600-cells) and then doubling the number of cells on both dimensions (80x3200-cells), we observe differences in temperature along the first 25 % of the domain length which do not overpass 0.09 K (not shown). Despite such a weak impact, this increase in mesh resolution allows a change of about 5 % in swelling degree and 50 % in suspension viscosity estimates. The 80x3200-cells mesh is assumed in the remaining of this study.

All the results discussed above were obtained by assuming the value D_S = 1e-12 $m^2.s^{-1}$ for the coefficient of diffusion required in the second-order kinetics equation (7). In other words, our numerical model was able to reach convergence by assuming such a D_S value. Nevertheless, no convergence was reached for D_S values below 5e-13 $m^2.s^{-1}$ even in the case of the (best present) 80x3200-cells mesh. Such values are one to two orders of magnitude higher than the estimative provided by the theory of diffusion in colloidal suspensions (see Section 2). An additional set of sensitivity tests was hence conducted, in order to assess the dependence of our results with the coefficient of diffusion.

Figure 3 compares swelling degree and suspension viscosity estimates at the heating wall for three D_S values, for the aspect ratio dz/dr = 5 and the mesh constituted of 80x3200 cells. Almost full swelling takes progressively place along the first 1/4 of the domain's length. Red curves correspond to D_S = 1e-12 $m^2.s^{-1}$. Gray symbols correspond to results obtained by assuming a coefficient of diffusion twice this value (D_S = 2e-12 $m^2.s^{-1}$). After such an increase, granule swelling is slightly delayed with respect to the previous condition: the swelling degree 75 % is reached after about 7 % and no longer after 5 % of the domain's length. The suspension viscosity decreases throughout the domain, e.g. by about 20 % at a distance of 0.1 m from the inlet. Opposite effects take place after dividing by two the former coefficient of diffusion: D_S = 5e-13 $m^2.s^{-1}$ (black symbols). Stronger effects on both swelling degree and suspension viscosity would be expected if we had reached numerical model convergence at still lower values for the coefficient of diffusion; if we had divided by 100 the value D_S = 1e-12 $m^2.s^{-1}$, the theoretical value provided by equation (9) would be approached.

The numerical representation of coupled processes is difficult at the heating wall because the high magnitude of thermal and velocity gradients which prevail there: fluid particles are associated with vanishing velocity, and they are directly exposed to the heating power. Hence, both granule swelling and suspension viscosity are expected to increase sharply from their starting values near the corner of the domain inlet with the heating wall. Our present calculation capabilities allow model convergence and consistent results for a mesh no finer than about 80x3200-cells, after assuming a coefficient of diffusion no smaller than 5e-13 $m^2.s^{-1}$. Results discussed hereafter were obtained under such conditions.

The left section of Fig. 4 shows temperature (top), swelling degree (center) and suspension viscosity (bottom) fields resulting from the simulations described above. The suspension viscosity field was deformed according to the velocity, and inlet and outlet velocity profiles can be appreciated. Dark blue and red colors correspond to the respective minimum and maximum values: 293.15 < T < 364.18 K, zero < S < 0.9996, and 6.911e-4 < η <7.105e-3 Pa.s. The food product is heated from the wall (bottom of domain). Fluid particles move slower and reach higher temperatures when running near it. Starch granules swell after heating; as a consequence, their volume fraction increases and also the suspension viscosity. In comparison with the conditions prevailing near the domain inlet, the suspension viscosity increases by a factor of about 7 near the corner of the domain outlet with the heating wall, slowing down the velocity in this region.

These results follow, in a partial extent, those obtained by Liao *et al*. (2000). Those authors also observed in the heating section of their tubular exchanger an increase of viscosity near the heating wall due to gelatinization, leading to a velocity decrease near this wall and a velocity increase at the axis of symmetry. Nevertheless starch type and concentration were different (4 % of waxy rice starch), and heating conditions were stronger (145°C) than those considered in our study; therefore a direct comparison of results seems difficult. Their maximum suspension viscosity was much higher (about 6 Pa.s), which caused velocity profiles almost flat were the food

product was very viscous; this was not observed in our case. Other geometries than tubular exchangers have been adopted in numerical models coupling fluid flow, heat transfer and starch gelatinization, like axially rotating cans (for instance, Tattiyakul *et al*. 2001). Any comparison with such results seems far to be straightforward.

The evolution of food product properties can also be studied with the help of hypothetical trajectories of fluid particles released at the domain inlet. We can imagine each fluid particle as a suspension droplet containing an ensemble of starch granules at similar thermodynamic and kinetic conditions. Figure 4 displays, in its right section, selected properties associated with fluid particles released at the domain inlet, at 0.5 mm and at 1 mm from the heating wall. Because the maximum velocity takes place at the axis of symmetry, the residence time corresponds to about 86 and 36 s, respectively. When reaching the domain outlet, fluid particles released at 0.5 mm are associated with higher values of temperature, mean diameter, and suspension viscosity than particles released at 1 mm from the heating wall. Other the granule starch swelling, the suspension viscosity depends on the continuous phase (pure water) viscosity. The latter slowly decreases with heating, and this fact explains why the suspension viscosity is slightly reduced during the first seconds after particle release.

Positions A and B in Fig. 4 were chosen because they correspond to a same temperature value (about 66 °C). Position A represents the outlet for fluid particles released at 1 mm from the heating wall; they reached this position after running about 36 s since the inlet. Position B is located before the outlet; fluid particles released at 0.5 mm from the heating wall move slower and spent about 55 s to come there since the inlet. Despite the same temperature, position B corresponds to a mean diameter of starch granules that is about 10 % greater, and to a suspension viscosity about 45 % greater, than respective values at the position A. These differences are explained by the fact that fluid particles running at different distances from the heating wall move with different velocities and hence experience different temperature histories. We conclude that the influence of temperature on the suspension viscosity is not instantaneous. The food product viscosity depends on the continuous phase viscosity as well as on the starch granule volume fraction. The former depends on the present local temperature whereas the latter depends on the whole thermal history of respective fluid particles.

4. Summary and Future Work

Our aim was to demonstrate that coupling a granule swelling model with a fluid flow and heat transfer model can highlight what happens for a given starch suspension inside a tubular exchanger. With the help of the numerical model developed in this study, selected food product properties can be followed along fluid particle trajectories. Our results show that the degree of transformation inside a fluid particle of food product depends on its whole thermal history. Hence the temperature evolution along the fluid particle trajectories must be properly assessed when the food product viscosity depends on the degree of transformation.

A simple food product transformation was here considered (starch granules swelling). Future efforts will focus on coupling fluid flow and heat transfer with more complex food product transformation processes, like particles aggregation, mechanical granules fragmentation, and amylose solubilization.

References

Bird, R. B., W. E. Stewart, and E. N. Lightfoot, "Transport Phenomena (Revised Second Edition)". John Wiley & Sons, New York, 905pp (2007)

Done, D. and D. G. Baird, The effect of thermal history on the rheology and texture of thermotropic liquid crystalline polymers. *Polymer Engineering and Science*, **27**, 816-822 (2004)

Kuipers, J. A. M. and W. P. M. van Swaaij, Computational fluid dynamics applied to chemical reaction engineering. *Advances in Chemical Engineering*, **24**, 227-328 (1998)

Kumar, A. and I. Dilber, "Fluid flow and its modeling using computational fluid dynamics." In *Handbook of Food and Bioprocess Modeling Techniques*, S. S. Sablani, M. S. Rahman, A. K. Datta, and

A. S. Mujumdar (Eds.). CRC Press, Boca Raton, 41-83 (2007)

Lagarrigue, S., G. Alvarez, G. Cuvelier, and D. Flick, Swelling kinetics of wazy maize and maize starches at high temperatures and heating rates. *Carbohydrate Polymers*, **73**, 148-155 (2008)

Liao, H.-J., M. A. Rao, and A. K. Datta, Role of thermo-rheological behaviour in simulation of continuous sterilization of a starch dispersion. *Transactions of the Institution of Chemical Engineers*, **78C**, 48-56 (2000)

Liu, H., F. Xie, L. Yu, L. Chen, and L. Li, Thermal processing of starch-based polymers. *Progress in Polymer Science*, **34**, 1348-1368 (2009)

Norton, T. and D.-W. Sun, Computational fluid dynamics (CFD) - An effective and efficient design and analysis tool for the food industry: A review. *Trends in Food Science and Technology*, **17**, 600-620 (2006)

Schenk, O. and K. Gartner - 2004 - Solving unsymmetric sparse systems of linear equations with PARDISO. *Future Generation Computer Systems*, **20**, 475-487 (2004)

Silva, J. A. L. and J. A. P. Coutinho, Dynamic rheological analysis of the gelation behaviour of waxy crude oils. *Rheologica Acta*, **43**, 433-441 (2004)

Tattiyakul, J., M. A. Rao, and A. K. Datta, Simulation of heat transfer to a canned corn starch dispersion subjected to axial rotation. *Chemical Engineering and Processing*, **40**, 391-399 (2001)

Thomas, D. G., Transport characteristics of suspension. VIII: A note on the viscosity of Newtonian suspensions of uniform spherical particles. *Journal of Colloid Science*, **20**, 267-277 (1965)

Acknowledgements

The research leading to these results has received funding from the European Community's Seventh Framework Programme (FP7/ 2007-2013) under the grant agreement n° FP7-222 654-DREAM.

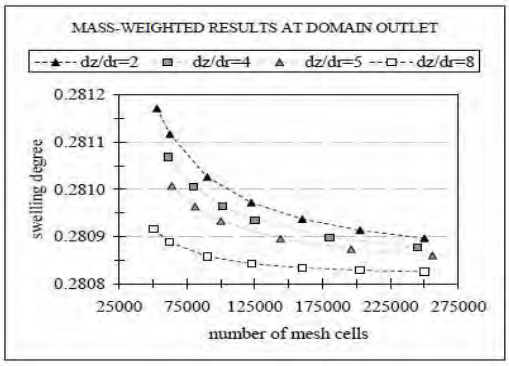

Figure 1. Mass-weighted results at the domain outlet, for selected values of the aspect ratio *dz/dr*. Dotted lines were included for presentation purposes only.

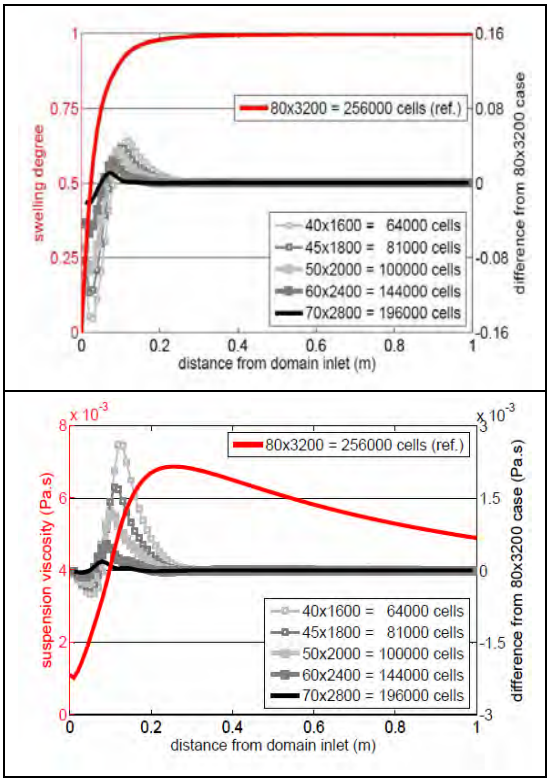

Figure 2. Selected results at the heating wall, as a function of the distance from the domain's inlet. Red symbols show results obtained with the 80x3200-cells mesh (values on left side). These latter are compared (differences on right side) with results obtained with gradually poorer resolution meshes (gray and black symbols).

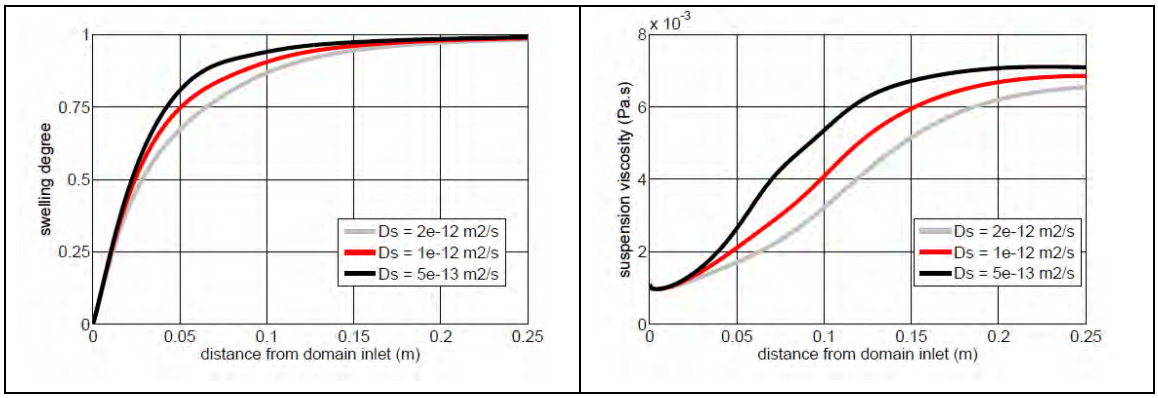

Figure 3. Selected results at the heating wall, for few values of the coefficient of diffusion assumed in representing the 2nd-order kinetics equation. Red curves correspond to D_S = 1e-12 $m^2.s^{-1}$ (results shown in Fig. 2); gray and black curves correspond to twice and half that value. All these results were obtained with the aspect ratio *dz/dr* = 5 and the 80x3200-cells mesh. Only the first 1/4 of the domain's length is displayed.

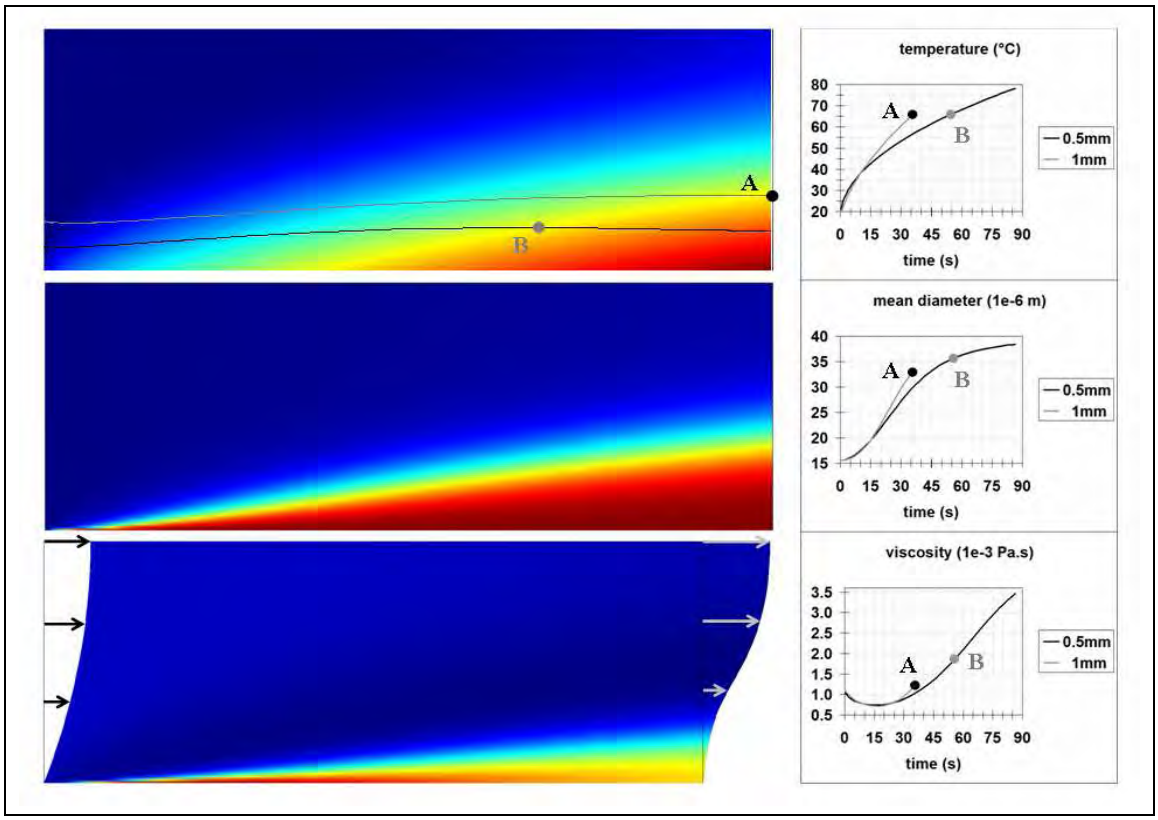

Figure 4. Main results provided by the numerical model. Left section presents the temperature (top), swelling degree (center) and suspension viscosity (bottom) fields; inlet is on the left, heating wall is on the bottom. Dark blue and red colors correspond to the respective minimum and maximum values: 293.2 < T < 364.2 K, 0 < S < 0.9996, and 6.911e-4 < η <7.105e-3 Pa.s . Right section presents the time series of selected properties corresponding to two trajectories followed by hypothetical fluid particles released at the inlet at 0.5 and 1 mm from the heating wall (see text).